Bioprocess Biosyst Eng (2016) 39:1163–1172
DOI 10.1007/s00449-016-1592-y

ORIGINAL PAPER

The nanofibrous PAN-PANi scaffold as an efficient substrate for skeletal muscle differentiation using satellite cells

Simzar Hosseinzadeh[1,3] · Matin Mahmoudifard[2,3] · Farzaneh Mohamadyar-Toupkanlou[3] · Masomeh Dodel[3] · Atena Hajarizadeh[4] · Mahdi Adabi[1] · Masoud Soleimani[3,5]

Received: 2 November 2015 / Accepted: 14 March 2016 / Published online: 16 April 2016

Abstract Among polymers, polyaniline (PANi) has been introduced as a good candidate for muscle regeneration due to high conductivity and also biocompatibility. Herein, for the first time, we report the use of electrospun nanofibrous membrane of PAN-PANi as efficient scaffold for muscle regeneration. The prepared PAN-PANi electrospun nanofibrous membrane was characterized by scanning electron microscopy (SEM), Attenuated total reflectance fourier transform infrared spectroscopy (ATR-FTIR) and tensile examination. The softer scaffolds of non-composite electrospun nanofibrous PAN govern a higher rate of cell growth in spite of lower differentiation value. On the other hand, PAN-PANi electrospun nanofibrous membrane exposed high cell proliferation and also differentiation value. Thank to the conductive property and higher Young's modulus of composite type due to the employment of PANi, satellite cells were induced into more matured form as analyzed by Real-Time PCR. On the other hand, grafting of composite nanofibrous electrospun scaffold with gelatin increased the surface stiffness directing satellite cells into lower cell proliferation and highest value of differentiation. Our results for first time showed the significant role of combination between conductivity, mechanical property and surface modification of PAN-PANi electrospun nanofibers and provid new insights into most biocompatible scaffolds for muscle tissue engineering.

Graphical abstract The schematic figure conveys the effective combination of conductive and surface stiffness on muscle tissue engineering.

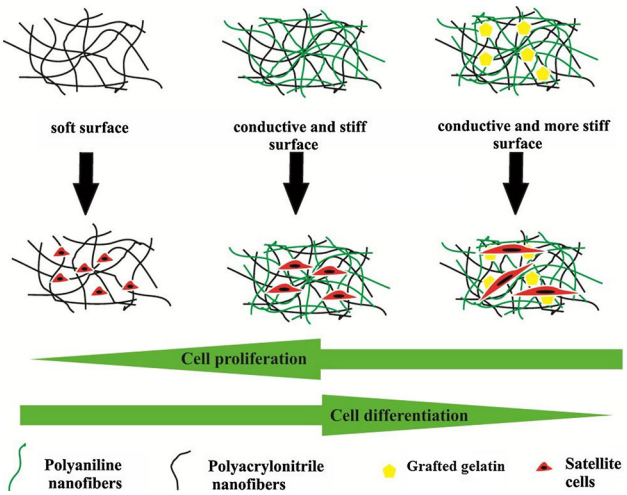

Keywords Polyaniline · Nanofibers · Conductive scaffolds · Surface stiffness · Satellite cells

✉ Masoud Soleimani
soleim_m@modares.ac.ir

Simzar Hosseinzadeh
s_hosseinzadeh@razi.tums.ac.ir

[1] Department of Medical Nanotechnology, School of Advanced Technologies in Medicine, Tehran University of Medical Sciences, Tehran, Iran

[2] Institute for Nanoscience and Nanotechnology, Sharif University of Technology, Tehran, Iran

[3] Nanotechnology and Tissue Engineering Department, Stem Cell Technology Research Center, Tehran, Iran

[4] Molecular Biology Department, Stem Cell Technology Research Center, Tehran, Iran

[5] Department of Hematology, Faculty of Medical Sciences, Tarbiat Modares University, Tehran, Iran

Introduction

Fabrication of biocompatible scaffolds to mimic the external cellular matrix (ECM) is one of the most attractive trends in tissue engineering (TE) field. An appropriate scaffold for a special tissue should render specific requirements for the growth and proliferation of a specific cells [1]. Materials used for such scaffolds should own proper mechanical and electrical properties beside chemical and biological compatibilities [2–4]. Many conducting polymeric composite scaffolds were reported previously which offer good cell growth and differentiation [5, 6]. Conducting scaffolds improve the propagation of electrical signal throughout the engineered cardiac tissue [7, 8]. It has been reported that electrical conductive scaffolds are proper to stimulate muscle [7], bone [6] and cardiac tissues [9].

To date, PANi is one of the most attracting conducting polymers with high level of chemical stability. Thanks to the simple oxidative polymerization and excellent electrical conductivity of PANi [10], considerable attention was attracted to apply PANi in many fields of science and technology including microwave absorption [11], chemical sensors [12], corrosion protection coatings [7] electromagnetic interference (EMI) shielding [13], hydrogen storage [14], rechargeable batteries [15] and biomedical applications [16, 17].

PANi has five different oxidation forms namely leucoemeraldine, protoemeraldine, emeraldine, nigraniline and pernigraniline.

Emeraldine is the most applicable form of PANi because of its high stability at room temperature and has two distinguished forms: insulator form (emeraldine base (EB)) and conducting form [emeraldine salt (ES)] [18]. By doping of PANi with organic acids like camphor sulfuric acid (CSA), the EB can be dissolved in common organic solvents. Moreover, high level of electrical conductivity up to 1–100 S/cm can be obtained [19, 20].

On the other hand, polyacrylonitrile (PAN) fibers have been found its place in many high tech applications such as water absorbents, ion exchange materials and precursors for the production of carbon fibers. One of the main reasons for versatility of these fibers in wide range of applications is due to the presence of high thermal stability [21, 22].

In addition to conventional fiber spinning technique like wet spinning and dry spinning, electrospinning technique provides new chance for the researchers to produce fine fibers with wide range of diameter from different materials.

The electrospun nanofibrous membranes are one of the best candidate for versatile applications including tissue engineering, filtration, reinforcement in composite materials, fuel cells, hydrogen storage, sensors, and batteries [23–25].

In the present study, first of all we report the synthesis of PAN-PANi composite nanofibrous membrane by electrospinning process. The effects of adding PANi to PAN solution on the morphological, mechanical and electrical properties of the electrospun PAN-PANi composite nanofibers were studied in the following. After that, for the first time, we used the corresponding electrospun mat as a scaffold to investigate the ability of this membrane for the proliferation and differentiation of satellite muscle stem cell.

Materials and methods

Preparation of nanofibrous scaffolds and characterizations

PANi (Poly aniline) (Aldrich 25233-30-1) with an average molecular weight of ca 100,000 Da and CSA (Camphor sulfonic acid) (Aldrich 5872-08-2) were used as the conductive polymer and dopant agent, respectively. Also, PAN (Poly acrylonitrile) (Aldrich 25014-41-9) with the average molecular weight of ca 100,000 Da was exploited due to electro active property in concentrations as described below briefly. PANi (5 g/1000 ml) and CSA (5 g/1000 ml) were dissolved in DMF and stirred vigorously for 3–4 h at room temperature (RT). The obtained solution was filtered off and blended with PAN (100 g/1000 ml of DMF) at ratio of PAN-PANi 70/30 v/v by mixing for 2 h at room temperature (RT).

PAN-PANi nanofibrous membranes were fabricated via electrospinning technique according to following parameter.

The distance between needle and collector was adjusted to 16 cm. The solution was ejected from needle by a syringe pump. High voltage of 15 kV was applied between the nozzle and collector to force the solution droplet from the needle and fabrication of fine fibers with the nanometer diameter on the collector. The flow rate of electrospinning was set to 0.3 ml/hr.

Characterization of composite PAN-PANi and non-composite PAN solutions and electrospun forms

The conductivity and the viscosity of PAN and PAN-PANi solutions were measured by a conductivity meter (Jenway, 4010) and a Rheometer (Brookfield, DV-II+Programable) respectively. The fiber morphology of composite and non-composite nanofibrous membrane was studied before and after cell seeding using a scanning electron microscope (SEM, Philips XL30, Netherlands). The mean, standard deviation and standard error diameter of nanofiber were

calculated by image j software based on the SEM images. For each sample, 25 nanofiber in SEM images was chosen and their diameter was measured. Attenuated Total Reflection Fourier Transform (ATR-FTIR Thermo Nicolet model: NEXUS 670, USA) was used to investigate the chemical characteristics of membrane. The ATR-FTIR spectra were recorded for 600–4000 cm^{-1}.

Mechanical properties of fabricated membranes were also tested at a 50 mm/min crosshead speed of regarding machine [SANTAM (Iran, SPM20)]. To measure the thickness of electrospun samples, they were cut in a rectangular shape of 10 mm wide with 60 mm length and a digital micrometer was used. A force of 0.5 kN was applied to the specimens and stress–strain curve was recorded accordingly.

The peak stress (tensile strength), strain and Young's modulus (E) were calculated using following formulas:

$$\text{Peak stress (MPs)} = F/A \quad (1)$$

where F is the maximum load of force (Newton) and A (squared meter) is the cross-sectional area of samples.

$$\text{Strain } (\%) = (L - L0)/L0 \times 100 \quad (2)$$

$L0$ is the initial length of the sample and L denotes the elongated length dimension at the break point of the sample. The Young's modulus (elastic modulus) was determined from the slope of the stress–strain curve in the elastic region [26].

The isolation of satellite cells and characterization of their proliferation and differentiation

The enrichment of satellite cells was carried out based on the previously reported procedure of pre-plating technique [27]. Figure 1 schematically shows the isolation procedure of satellite cells. Briefly, the 10-day-*NMRI* mice were killed, and skeletal muscles were obtained from their fore and hind feet. Non-muscle tissues were gently removed, then we added Trypsin (0.25 % Trypsin/1 mM EDTA) (Gibco) for 4 min. For complete digestion of sample, enzymatic dissociating solution including of collagenase type1 (Gibco), collagenase type 4 (Gibco) 0.1 % and dispase 1.75 unit/mg (Gibco) were used for an overnight at 4 °C. After 24 h, the sample was incubated for 3.5 h at 37 °C on a shaker and was filtered through a 70 μm mesh (BD Falcon). This suspension was centrifuged at 1250 rpm for 5 min, and the isolation process was followed by removing the supernatant. Finally, the obtained cells were incubated for 1.5 h and pre-plated as a first step. The pre-plating procedure was repeated for 6 times with one for each day. For each pre-plating, the suspended cells and low adherent cells were transferred into a gelatin (Sigma)-coated flask containing medium of DMEM-high F12 and 10 % FBS. The enriched cells from 6th-pre-plate were used for seeding onto prepared nanofibrous scaffolds. Figure 2 presents the related figures with the all cell types which were obtained cells from digestion (a) and isolated cells from pre-plating 6 (b).

As-prepared scaffolds were cut in desired size and incubated in 70 % filtered ethanol for 1 h. The ethanol was aspirated and replaced with media culture for 24 h prior to cell seeding. The isolated satellite cells by pre-plating technique were counted and seeded on the corresponding scaffolds.

The isolated cells were cultured in DMEM-high/F12 (Gibco) with 10 % FBS and seeded with an initial density of 10×10^3 cells/cm^2 onto non-composite and composite type of prepared scaffolds including plasma-treated PAN and plasma treated PAN-PANi electrospun mats with and without presence of gelatin. The cell culture media was added after 30 min, after the enough time had passed for cell adhesion on scaffolds.

The cells which were cultured on plasma-treated PAN nanofibrous scaffold were used as the control group.

4′, 6-diamidino-2-phenylindole (DAPI, Sigma) staining was carried out based on the previously reported protocol for the determination of nuclear localization, [28] and treated scaffolds were studied under a fluorescence microscopy (Nikon, Eclipse TE2000-S, Japan).

The viability of cells was evaluated on 1, 4, 11, and 15th day after seeding of satellite cells using MTT (3-[4,5-dimethylthiazol-2-yl]-2,5-diphenyl tetrazolium bromide). Each cell-cultured scaffolds were rinsed by PBS and incubated at 37 °C for 3.5 h with MTT dissolved in medium of DMEM without FBS. The MTT solution was

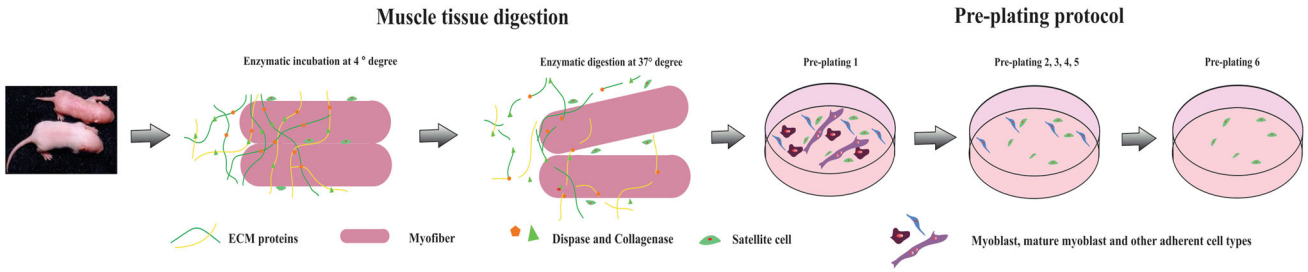

Fig. 1 The isolation procedure of satellite cells from mice skeletal muscle using pre-plating technique

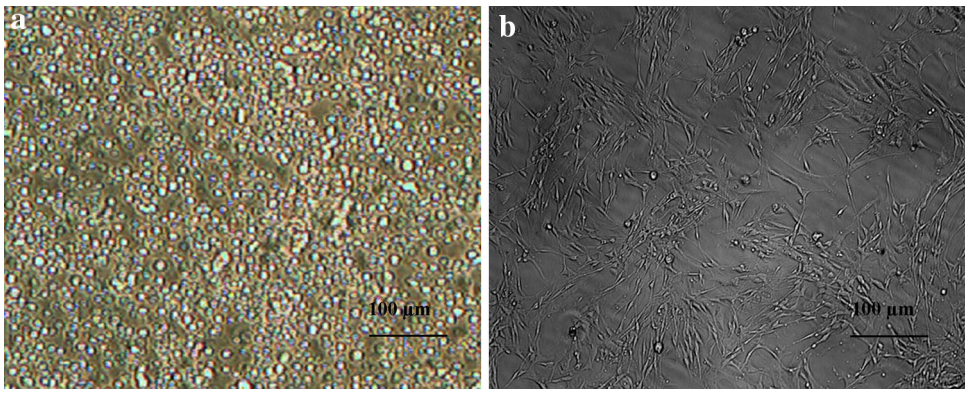

Fig. 2 **a** The all type of isolated cells from skeletal muscle after digestion period and **b** The enriched population of satellite cells after 6th pre-plating

aspirated and electrospun mats were incubated in DMSO at 37 °C, and the production of formazan crystals was quantified by absorbance measurement at 570 nm. The cell growth rate was calculated according to formula (3) [29]:

$$\text{Relative growth } (\%) = (\text{Absorbance of PAN - PANi scaffold})/(\text{Absorbance of plasma treated PAN scaffold}) \times 100 \quad (3)$$

Real-Time PCR was performed 15 days after seeding of satellite cells to evaluate the role of corresponding scaffolds on the maturation of satellite cells. Here, β-actin was used as the internal control and Pax7, MyoD, α-actin, MyH, M-cadherin, and CD34 as skeletal muscle marker genes.

TRIzol reagent (Sigma) was used to isolate total RNA. cDNA was synthesized with M-MuLV reverse transcriptase (RT) and Random Hexamer primers, according to the manufacturer's instructions (Fermentas). The PCR reactions (94 °C as annealing temperature for 3 min and 35 cycles at 94° for 30 s, 62° for 45 s, 72° for 45 s followed by extension time of 72° for 7–10 min) were conducted with 0.5 µl cDNA product.

Real-Time PCRs were carried out using Maxima™ SYBR Green/ROX Real-Time PCR Master Mix (Fermentas), and Rotor-gene Q software (corbett) was used to analyze the average of threshold cycle. Gene expression levels were calculated based on comparative Ct method.

The difference between data was studied between the plasma treated PAN as control group and PAN-PANi types as experimental groups.

T test student was used to assess differences between results of composite and non-composite electrospun scaffolds and the *p* value of less than or equal with 0.05 and 0.01 were interpreted as being significant. One and two asterisk indicates the statistical difference with *p* value of ≤ 0.05 and 0.01, respectively. The whole data are shown in curves areas as mean ± standard error.

Results

The fiber diameter of electrospun nanofibrous membranes of PAN and PAN-PANi by SEM and conductive property of regarding solutions

The morphology characterization of nanofibrous membrane by SEM was shown in Fig. 3. The SEM examinations confirmed the presence of a micrometric distance between fiber-to-fiber with the nanofibrous electrospun membranes introducing the presence of porous structure within the

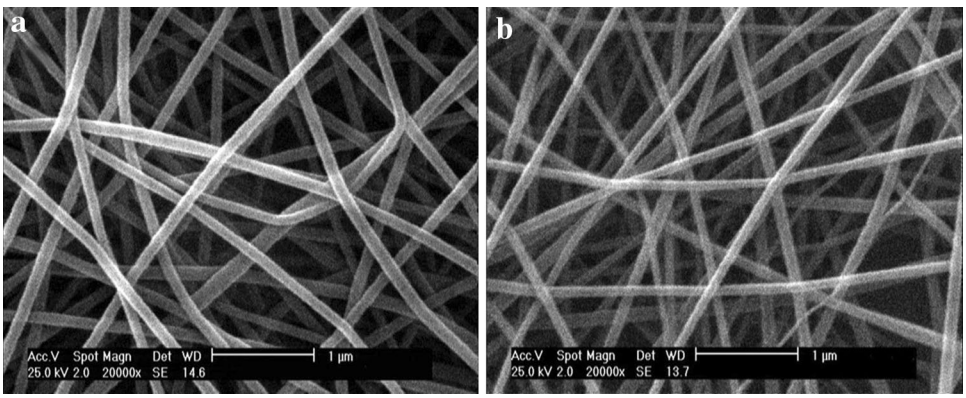

Fig. 3 SEM micrographs of beadless nanofibers which were produced using electrospining of PAN (**a**) and PAN-PANi (**b**)

Table 1 The changes in viscosity and conductivity values of composite (PAN-PANi) and non-composite solutions (PAN) at 26 °C

Sample	Viscosity (mPa.s)	Conductivity (μs/cm)	Diameter (nm)
DMF	–	4.56 ± 0.04	–
PAN	1426.22 ± 14.13	0.62 ± 0.09	149.51 ± 18.80
PAN-PANi	499.31 ± 18.10	38.58 ± 0.09	116.7 3 ± 25.42

prepared non-woven mats. Moreover, it can be seen from Table 1, with addition of PANi to PAN solution, a significant decrease in the viscosity and increase in conductivity are observed accordingly. Thus, the diameter of resulted nanofibers with electrospun PAN was altered after the addition of PANi from 149.5 ± 18.8 nm to 116.7 ± 25.4 nm.

The characterization of mechanical properties for PAN and PAN-PANi nanofibers

Figure 4 and Table 2 show the representative stress–strain curves and data of the electrospun PAN and PAN-PANi nanofibers. The typical stress–strain response of electrospun PAN nanofibers exhibited a linear elastic behavior up to 2.5 % deformation with a young's modulus E of 74.93 MPa and deformation at the break point of about 14.11 %. However, the mechanical property of composite PAN-PANi nanofibrous membrane changed compared to PAN nanofibrous membrane due to the presence of PANi component. The linear elastic parameter and young's modulus of composite PAN-PANi nanofibrous membrane were shifted to nearly 0.27 % and 146.19 MPa, respectively. Also, the breaking point was replaced to 56.26 %.

ATR-FTIR assessment for characterization of non-woven scaffolds

The chemical characteristics of the different nanofibrous membrane including non-plasma treated PAN-PANi, plasma treated PAN-PANi, gelatin-grafted plasma treated PAN-PANi and non-plasma treated PAN were studied using ATR-FTIR and their spectra shown in Fig. 5.

Bands at 3100–3600 cm^{-1} which are almost attributes to O–H vibration [30], showed a higher intensity after grafting with gelatin. This band is in accordance with –OH stretching vibration of carboxylic acid [31] with the prepared nanofibrous membrane. The corresponding functional groups which were resulted as a function of oxygen plasma process became sharper after gelatin grafting process. The noted peaks were disappeared with non-plasma treated types of PAN and PAN-PANi nanofibrous

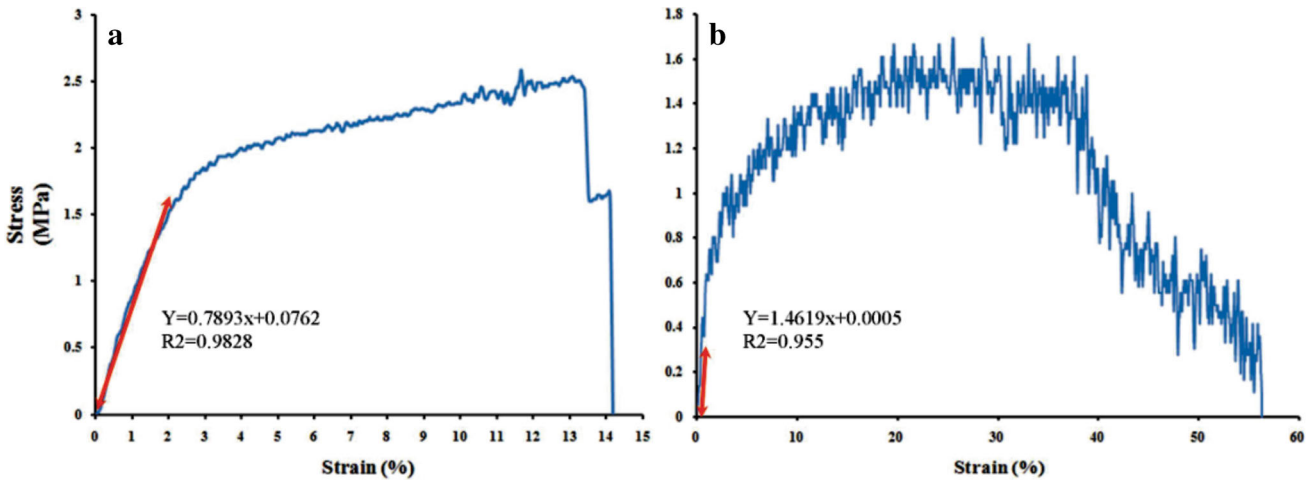

Fig. 4 Stress–strain response of electrospun nanofibers of PAN (**a**) and PAN-PANi (**b**)

Table 2 Mechanical properties of composite (PAN-PANi) and non-composite (PAN) fabricated scaffolds

Samples	Peak stress (MPa)	Break strain (%)	Young's modulus (MPa)
PAN nanofibrous scaffold	2.51 ± 0.59	14.11 ± 0.98	74.93 ± 2.41
PAN-PANi nanofibrous scaffold	1.69 ± 0.11	56.26 ± 3.41	146.19 ± 7.22

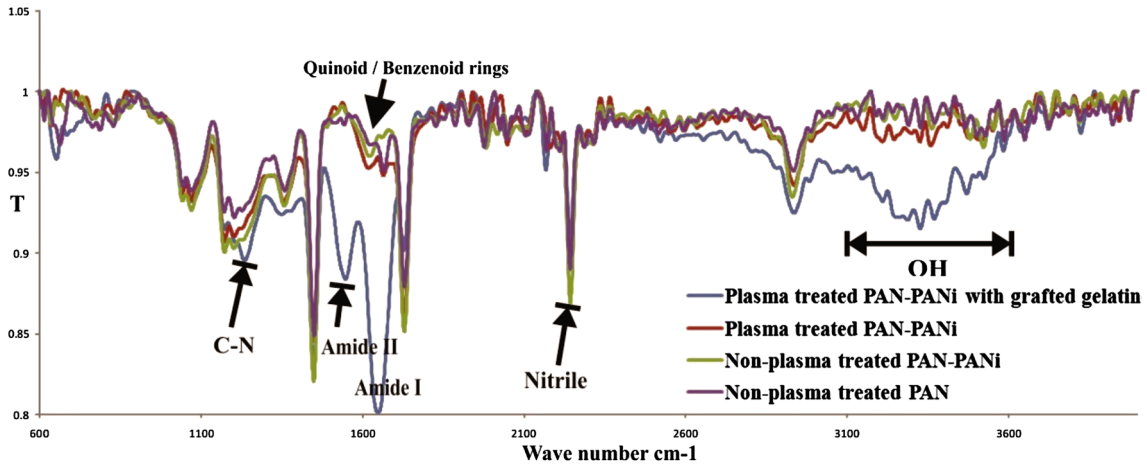

Fig. 5 FTIR-ATR spectra of electrospun nanofibers samples including non-plasma treated of PAN, non-plasma and plasma-treated of PAN-PANi with and without grafted gelatin

membranes. The band at 1234 cm^{-1} which was increased after grafting with gelatin, is the representative of the C–N stretching of a secondary aromatic amine [32]. After gelatin-immobilization, new peaks at 1661 cm^{-1} [33], 1550 cm^{-1} [33, 34], and 3302 cm^{-1} [35] were observed originated from the amide I, amide II and amine bands, respectively. The amine band was overlapped with the region of –OH stretching vibration. Another peak was observed in the range of 2246 cm^{-1} related to nitrile bonds (C≡N) of PAN fibers [36]. Furthermore, the exposed band at nearly 1600 cm^{-1} is the characteristic peak of quinoid ring of PANi [37].

SEM examinations for cell morphological study and MTT assay for growth rate of satellite cells on composite and non-composite scaffolds

The SEM micrographs of prepared nanofibrous mats were studied after 15 days of cell seeding and presented in Fig. 6. Higher count of extended cells on non-composite

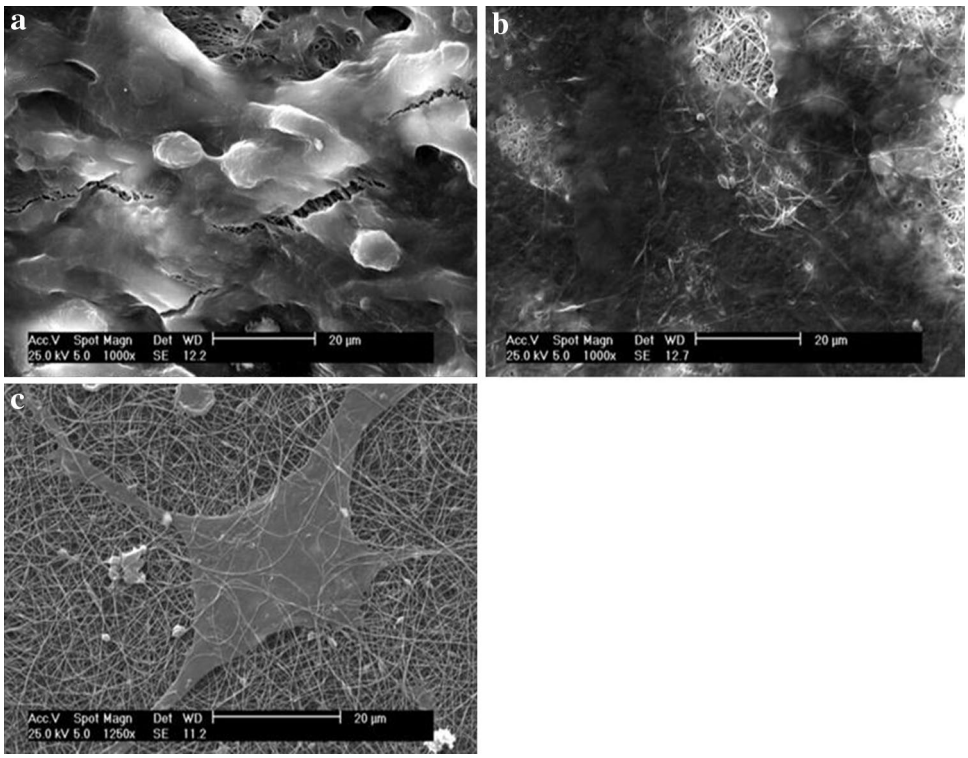

Fig. 6 SEM micrographs of satellite cells seeded on plasma treated electrospun nanofibers of PAN (**a**), plasma-treated electrospun nanofibers of PAN-PANi (**b**) and gelatin-grafted plasma-treated electrospun nanofibers of PAN-PANi (**c**) after 10 days of cell culture

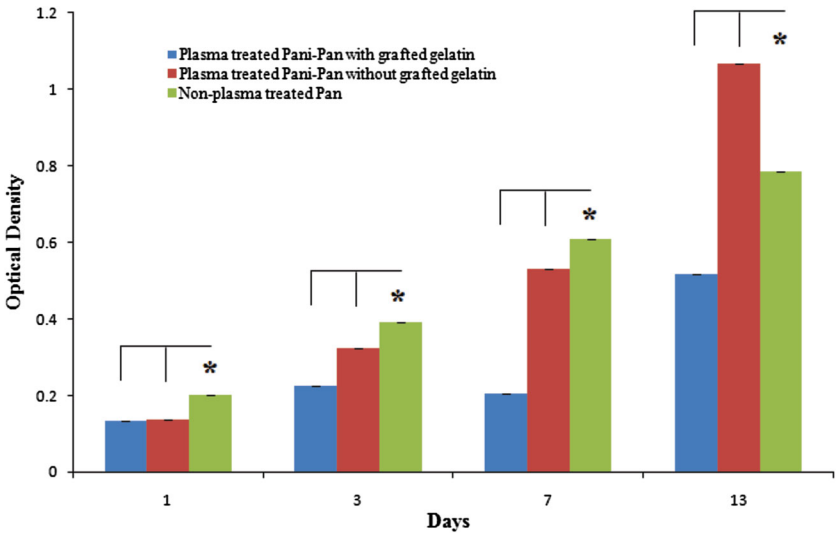

Fig. 7 Cell viability of cultured satellite cells on plasma treated electrospun nanofibers of PAN, plasma-treated electrospun nanofibers of PAN-PANi and gelatin grafted plasma-treated electrospun nanofibers of PAN-PANi after 1, 3, 7 and 13 days of cell culture

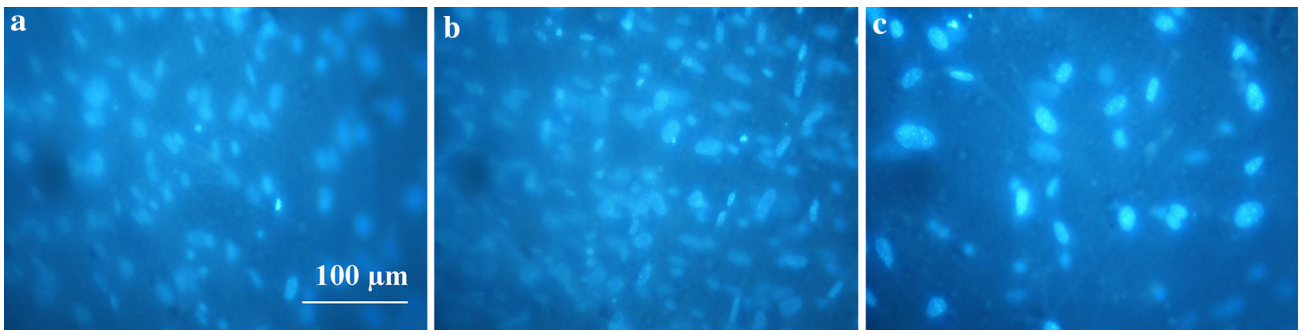

Fig. 8 DAPI staining of satellite cells seeded on plasma-treated electrospun nanofibers of PAN (**a**), plasma-treated electrospun nanofibers of PAN-PANi (**b**) and gelation-grafted plasma-treated electrospun nanofibers of PAN-PANi (**c**) after 10 days of cell culture

electrospun nanofibers of PAN and non-gelatin grafted composite type of PAN-PANi scaffold is observed. However, glatin-grafted plasma treated PAN/PANi nanofibrous scaffold provided better cell spreading as result of more stiffness.

The results of MTT assessment are given in the form of mean and standard deviation at days 1, 3, 7, and 13, and shown in Fig. 7. With comparison between the absorbency values of corresponding scaffolds, it was revealed that there is a significant difference between PAN-PANi groups and PAN type behavior over cell culture ($p \ll 0.05$). Moreover, MTT assay indicated the relative growth of seeded cells on gelatin-grafted PAN-PANi nanofibrous scaffolds as 66.08, 57.2, 33.7, and 65.9 % and non-gelatin grafted type as 67.5, 82.6, 87.1, and 135.4 % for 1, 3, 7, and 13th day after cell seeding, respectively. The corresponding data obey the first grade cytotoxicity for values between 75 and 99 %, second grade for values of 50–74 % and third grade for values between 25 and 49 % [29].

Moreover, DAPI staining defended the obtained results of SEM analysis and MTT assay. As it can be observed in Fig. 8, satellite cells showed higher cell number with non-composite nanofibrous membrane of PAN and non-gelatin grafted composite type of PAN-PANi compared to gelatin-grafted composite one.

The differentiation value of satellite cells by Real-Time-PCR

Real-Time PCR was performed for the determination of muscular markers in the differentiation phase and presented in Fig. 9. The primers which are listed in Table 3, included a set of primers: the transcription factors (MyoD), contractile apparatus of muscle cells (Myosin Heavy Chain; MyH, α-sarcomeric actin) which were normalized with β-actin (the housekeeping gene in skeletal muscle cells). The gene expression profile was assessed in three separated groups including: the cells which were cultured

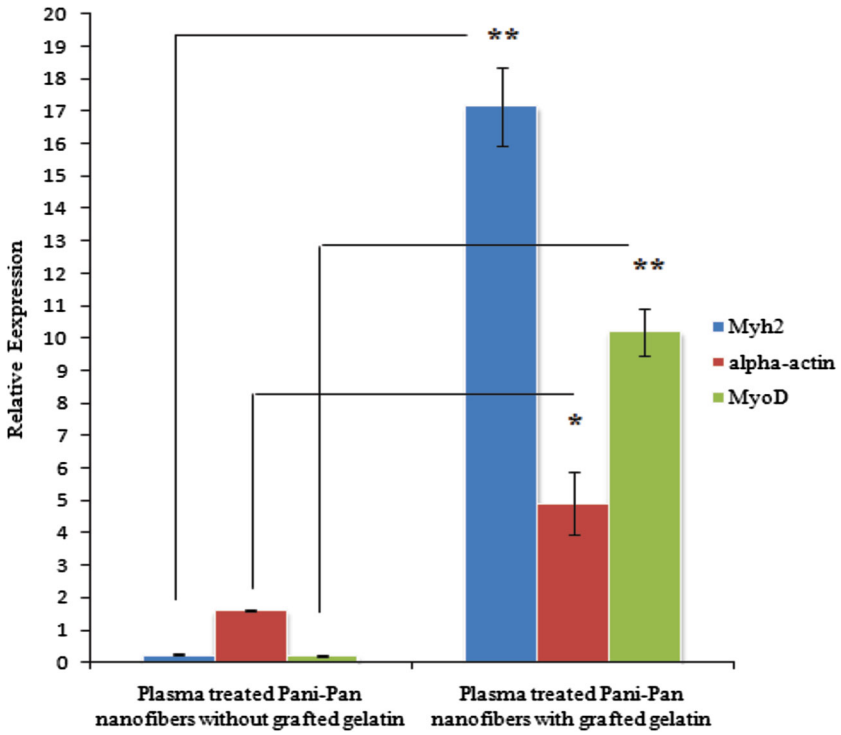

Fig. 9 The Real-Time PCR shows relative expression of Markers for satellite cells on gelatin-grafted plasma-treated PAN-PANi and non-gelatin grafted plasma-treated PAN-PANi nanofibers which were calibrated using the values of plasma treated electrospun nanofibers of PAN as control group

Table 3 The list of primers used for investigation of gene expression using Real-Time PCR

Primers	Forward (5′–3′)	Reverse (5′–3′)
MyH	GCTTACTTACCAGACAGAAGAAG	TGTTCCTCAGCCTCCTCAG
Myo D	CTGATGGCATGATGGATTAC	GACACAGCCGCACTCTTC
α-sarcomeric actin	GTGGCTATTCCTTCGTGAC	GCAGACTCCATACCGATAAAG
M-cadherin	AGGTGGTGGCTGTGTATAATC	GCCTCCATAAAGAACTCATCC
CD34	GCCAATAGCACAGAACTTCC	GCCAGCAGAACTCCAGAGG
Pax7	GCGTAAGCAGGCAGGAG	ATGGTTGATGGCGGAAG
Beta-actin as internal control	GTCCTCTCCCAAGTCCACAC	GGGAGACCAAAAGCCTTCAT

on gelatin-grafted of plasma treated PAN-PANi nanofibrous mat, non-gelatin grafted of plasma treated PAN-PANi type and plasma treated PAN nanofibrous mat. It should be mentioned, the gene expression value of both PAN-PANi groups was calibrated with the values of PAN nanofibrous scaffold. For all groups, the assessments were obtained after 15 days of cell seeding that the rate of cell proliferation showed the extreme value on the basis of MTT assay.

All mentioned skeletal muscle markers showed the higher expression rate with PAN-PANi electrospun scaffolds compared to PAN type. Moreover, gelatin grafted group of plasma treated PAN-PANi nanofibrous membrane confirmed the higher level of corresponding genes compared to non-gelatin grafted plasma treated PAN-PANi type.

Discussion

In the electrospinning process, the solution viscosity and conductivity are the two important parameters which can affect the electrospun nanofibers morphology. As reported previously, the average diameter of nanofibers reduces with decreasing the viscosity and increasing the conductivity of the electrospinning solution [38]. Herein, the addition of PANi to PAN solution decreases the fiber diameter significantly as a function of lower viscosity and higher conductivity. The resulted nanofibers mimic the size scale of extracellular matrix applying high surface area to volume ratio for more cell interactions and also favorable differentiation. Moreover, the obtained higher value of young's modulus and also lower percentage of elastic behavior with PAN-PANi nanofibrous membrane were

resulted as a function of the interactions between PAN and PANi in composite form (see Table 1). Thus, based on the results obtained from mechanical examination, the non-composite electrospun scaffold of PAN provided a softer substrate in comparative to composite type of PAN-PANi. As before reported [39], muscle stem cells tend to proliferate stronger on soft surfaces than stiff type. Thus, the non-gelatin grafted PAN-PANi electrospun nanofibrous scaffold as a soft substrate elucidates a lower ratio of cell growth compared to non-composite scaffold. Moreover, cell proliferation of non-gelatin grafted PAN-PANi electrospun nanofibrous scaffold was higher than gelatin grafted form of composite type. This is in consistent with the previous study that has introduced gelatin as a factor for increase of surface stiffness [40]. Hence, the grafting of scaffolds with gelatin reduces the cell spreading of satellite cells and also their proliferation rate while increases muscle differentiation.

The assessment with Real-Time PCR showed a higher value of MyoD as a proliferative and activation marker for satellite cells in gelatin-grafted samples compared with other groups. The up-regulate of corresponding marker approves the point of mature muscle cells into differentiation phase with overexpression of Myosin heavy chain (MyH) and α-sarcomeric actin [41]. It is obvious that the conductivity of PANi in composite electrospun nanofibers induces cell differentiation compared to non-conductive scaffold of PAN electrospun nanofibers. This is in agreement with other studies that have confirmed greater muscle differentiation of C2C12 myoblasts on electrospun scaffolds of poly(l-lactide-co-ε-caprolactone) (PLCL) and polyaniline (PANi) [9]. In spite of this, there is a sharp difference between two prepared conductive scaffolds including grafted and non-gelatin grafted of PAN-PANi electrospun nanofibers.

In our knowledge, gelatin which was grafted with PAN-PANi nanofibrous membrane, increases the stiffness property of related substrate into the higher value that supports cell differentiation drastically (see Graphical abstract). This is in agreement with other reports that have evaluated the influences of collagen fibrils on surface stiffness [40]. On the other hand, before studies confirm that stiffer surfaces induce more differentiation of muscle cells compared to softer one [42]. Precisely, it seems that the surface interactions of stiffer substrates like gelatin-grafted type of PAN-PANi nanofibrous membrane play a strong role for cell differentiation rather than cell proliferation. It should be mentioned that the presence of conductive polymer namely PANi governs the cell fate into muscle differentiation compared to non-composite PAN scaffold. Thus, a synergic differentiation is observed in combination between gelatin which was grafted on the surface of PAN-PANi nanofibrous mat and the presence of PANi as a conductive polymer.

Conclusion

In conclusion, it was found in this study that PAN-PANi composite electrospun nanofibers provides a more biocompatible substrate compared to non-composite PAN electrospun membrane as a function of conductive character and also higher Young's modulus value. On the other hand, grafting of corresponding composite scaffolds with gelatin remarkably increases the stiffness value of surface and direct cell differentiation into myogenic rout rather than cell proliferation. Furthermore, the presence of porous structure of fabricated nanofibrous membranes which can be observed from the SEM images can help to mimic ECM leading to more cell adhesion and favorable differentiation. In our knowledge, this study for first time highlights the combined effect of conductivity, mechanical properties of scaffold and also surface requirements for governing of muscle regeneration.

Acknowledgments This work was supported by a Grant of Stem Cell Technology Research Center, Tehran, Iran.

References

1. Bach A, Beier J, Stern-Staeter J, Horch R (2004) Skeletal muscle tissue engineering. J Cell Mol Med 8(4):413–422
2. Chen G, Ushida T, Tateishi T (2002) Scaffold design for tissue engineering. Macromol Biosci 2(2):67–77
3. Yan X, Chen J, Yang J, Xue Q, Miele P (2010) Fabrication of free-standing, electrochemically active, and biocompatible graphene oxide – polyaniline and graphene – polyaniline hybrid papers. ACS Appl Mater Interfaces 2(9):2521–2529
4. Sabir MI, Xu X, Li L (2009) A review on biodegradable polymeric materials for bone tissue engineering applications. J Mater Sci 44(21):5713–5724
5. Kai D, Prabhakaran MP, Jin G, Ramakrishna S (2013) Biocompatibility evaluation of electrically conductive nanofibrous scaffolds for cardiac tissue engineering. J Mater Chem B 1(17):2305–2314
6. Li N, Zhang X, Song Q, Su R, Zhang Q, Kong T et al (2011) The promotion of neurite sprouting and outgrowth of mouse hippocampal cells in culture by graphene substrates. Biomaterials 32(35):9374–9382
7. Ravichandran R, Sundarrajan S, Venugopal JR, Mukherjee S, Ramakrishna S (2010) Applications of conducting polymers and their issues in biomedical engineering. J R Soc Interface (**rsif20100120**)
8. Chen M-C, Sun Y-C, Chen Y-H (2013) Electrically conductive nanofibers with highly oriented structures and their potential application in skeletal muscle tissue engineering. Acta Biomater 9(3):5562–5572
9. Jun I, Jeong S, Shin H (2009) The stimulation of myoblast differentiation by electrically conductive sub-micron fibers. Biomaterials 30(11):2038–2047

10. Gittings J, Bowen C, Turner I, Baxter F, Chaudhuri J (2007) Characterisation of ferroelectric-calcium phosphate composites and ceramics. J Eur Ceram Soc 27(13):4187–4190
11. Dvir T, Timko BP, Brigham MD, Naik SR, Karajanagi SS, Levy O et al (2011) Nanowired three-dimensional cardiac patches. Nat Nanotechnol 6(11):720–725
12. Huang J (2006) Syntheses and applications of conducting polymer polyaniline nanofibers. Pure Appl Chem 78(1):15–27
13. Makeiff DA, Huber T (2006) Microwave absorption by polyaniline–carbon nanotube composites. Synth Met 156(7):497–505
14. Aussawasathien D, Dong J-H, Dai L (2005) Electrospun polymer nanofiber sensors. Synth Met 154(1):37–40
15. Ashassi-Sorkhabi H, Es'haghi M (2013) Electro-synthesis of nano-colloidal PANI/ND composite for enhancement of corrosion-protection effect of PANI coatings. J Mater Eng Perform 22(12):3755–3761
16. Jing X, Wang Y, Zhang B (2005) Electrical conductivity and electromagnetic interference shielding of polyaniline/polyacrylate composite coatings. J Appl Polym Sci 98(5):2149–2156
17. Srinivasan S, Ratnadurai R, Niemann M, Phani A, Goswami D, Stefanakos E (2010) Reversible hydrogen storage in electrospun polyaniline fibers. Int J Hydrogen Energy 35(1):225–230
18. Rehan H (2003) A new polymer/polymer rechargeable battery: polyaniline/LiClO 4 (MeCN)/poly-1-naphthol. J Power Sources 113(1):57–61
19. Hardy JG, Lee JY, Schmidt CE (2013) Biomimetic conducting polymer-based tissue scaffolds. Curr Opin Biotechnol 24(5):847–854
20. Veluru JB, Satheesh K, Trivedi D, Ramakrishna MV, Srinivasan NT (2007) Electrical properties of electrospun fibers of PANI-PMMA composites. J Eng Fibers Fabrics 2:25–31
21. Im JS, Kwon O, Kim YH, Park S-J, Lee Y-S (2008) The effect of embedded vanadium catalyst on activated electrospun CFs for hydrogen storage. Microporous Mesoporous Mater 115(3):514–521
22. Li M, Guo Y, Wei Y, MacDiarmid AG, Lelkes PI (2006) Electrospinning polyaniline-contained gelatin nanofibers for tissue engineering applications. Biomaterials 27(13):2705–2715
23. Saeed K, Haider S, Oh T-J, Park S-Y (2008) Preparation of amidoxime-modified polyacrylonitrile (PAN-oxime) nanofibers and their applications to metal ions adsorption. J Membr Sci 322(2):400–405
24. Giri Dev VR, Venugopal JR, Senthilkumar M, Gupta D, Ramakrishna S (2009) Prediction of water retention capacity of hydrolysed electrospun polyacrylonitrile fibers using statistical model and artificial neural network. J Appl Polym Sci 113(5):3397–3404
25. Dadvar S, Tavanai H, Morshed M (2014) Fabrication of nanocomposite PAN nanofibers containing MgO and Al2O3 nanoparticles. Polym Sci Ser A 56(3):358–365
26. Jeong SI, Jun ID, Choi MJ, Nho YC, Lee YM, Shin H (2008) Development of Electroactive and Elastic Nanofibers that contain Polyaniline and Poly (L-lactide-co-ε-caprolactone) for the Control of Cell Adhesion. Macromol Biosci 8(7):627–637
27. Gharaibeh B, Lu A, Tebbets J, Zheng B, Feduska J, Crisan M et al (2008) Isolation of a slowly adhering cell fraction containing stem cells from murine skeletal muscle by the preplate technique. Nat Protoc 3(9):1501–1509
28. Keane TJ, Londono R, Turner NJ, Badylak SF (2012) Consequences of ineffective decellularization of biologic scaffolds on the host response. Biomaterials 33(6):1771–1781
29. Liu Q, Wu J, Tan T, Zhang L, Chen D, Tian W (2009) Preparation, properties and cytotoxicity evaluation of a biodegradable polyester elastomer composite. Polym Degrad Stab 94(9):1427–1435
30. Toledano-Thompson T, Loría-Bastarrachea M, Aguilar-Vega M (2005) Characterization of henequen cellulose microfibers treated with an epoxide and grafted with poly (acrylic acid). Carbohydr Polym 62(1):67–73
31. Li F, Arthur EE, La D, Li Q, Kim H (2014) Immobilization of CoCl 2 (cobalt chloride) on PAN (polyacrylonitrile) composite nanofiber mesh filled with carbon nanotubes for hydrogen production from hydrolysis of NaBH 4 (sodium borohydride). Energy 71:32–39
32. Tang Q, Wu J, Sun H, Lin J, Fan S, Hu D (2008) Polyaniline/polyacrylamide conducting composite hydrogel with a porous structure. Carbohydr Polym 74(2):215–219
33. Nasir NM, Raha M, Kadri K, Rampado M, Azlan C (2006) The study of morphological structure, phase structure and molecular structure of collagen-PEO 600 K blends for tissue engineering application. Am J Biochem Biotechnol 2(4):175–179
34. Shabani I, Haddadi-Asl V, Seyedjafari E, Babaeijandaghi F, Soleimani M (2009) Improved infiltration of stem cells on electrospun nanofibers. Biochem Biophys Res Commun 382(1):129–133
35. Su C-Y, Lin C-K, Lin C-R, Lin C-H (2006) Polymerization-like grafting of thermoplastic polyurethane by microwave plasma treatment. Surf Coat Technol 200(10):3380–3384
36. Farsani RE, Raissi S, Shokuhfar A, Sedghi A (2009) FT-IR study of stabilized PAN fibers for fabrication of carbon fibers. World Acad Sci, Eng Technol 50:430–433
37. Khalid M, Tumelero MA, Brandt IS, Zoldan VC, Acuña JJ, Pasa AA (2013) Electrical conductivity studies of polyaniline nanotubes doped with different sulfonic acids. Indian J Mater Sci
38. Nasouri K, Shoushtari AM, Kaflou A, Bahrambeygi H, Rabbi A (2012) Single-wall carbon nanotubes dispersion behavior and its effects on the morphological and mechanical properties of the electrospun nanofibers. Polym Compos 33(11):1951–1959
39. Romanazzo S, Forte G, Ebara M, Uto K, Pagliari S, Aoyagi T et al (2012) Substrate stiffness affects skeletal myoblast differentiation in vitro. Sci Technol Adv Mater 13(6):064211
40. McDaniel DP, Shaw GA, Elliott JT, Bhadriraju K, Meuse C, Chung K-H et al (2007) The stiffness of collagen fibrils influences vascular smooth muscle cell phenotype. Biophys J 92(5):1759–1769
41. Zammit PS, Relaix F, Nagata Y, Ruiz AP, Collins CA, Partridge TA et al (2006) Pax7 and myogenic progression in skeletal muscle satellite cells. J Cell Sci 119(9):1824–1832
42. Ren K, Crouzier T, Roy C, Picart C (2008) Polyelectrolyte multilayer films of controlled stiffness modulate myoblast cells differentiation. Adv Funct Mater 18(9):1378